Available online at www.sciencedirect.com
SCIENCE DIRECT®
Advances in Space Research 35 (2005) 2037–2043
ADVANCES IN SPACE RESEARCH (a COSPAR publication)
www.elsevier.com/locate/asr

Characterization of the semi-annual-oscillation in mesospheric temperatures at low-latitudes

M.J. Taylor [a,*], A.K. Taori [a,1], D.R. Hatch [a], H.L. Liu [b], R.G. Roble [b]

[a] Center for Atmospheric and Space Science, Utah State University, 4415 Old Main Hill, Logan, UT 84322, USA
[b] NCAR, High Altitude Observatory, Boulder, CO, USA

Received 30 October 2004; received in revised form 27 May 2005; accepted 27 May 2005

Abstract

Novel measurements of the seasonal variability in mesospheric temperature at low-latitudes have been obtained from Maui, Hawaii (20.8°N, 156.2°W) during a 25-month period from October 2001 to January 2004. Independent observations of the OH (6, 2) Meinel band (peak height ~87 km) and the O_2 (0–1) atmospheric band emission (~94 km) were made using the CEDAR Mesospheric Temperature Mapper. The data revealed a coherent oscillation in emission intensity and rotational temperature with a well-defined periodicity of 181 ± 7 days. The amplitude of this oscillation was determined to be ~5–6 K in temperature and ~8–9% in intensity for both the OH and O_2 data sets. In addition, a strong asymmetry in the shape of the oscillation was also observed with the spring maximum significantly larger than the fall peak. These data provide new evidence in support of a semi-annual-oscillation in mesospheric temperature (and airglow emission intensities) and help quantify its seasonal characteristics.

Keywords: Airglow; Mesospheric temperature; Atmospheric oscillations; Seasonal variations

1. Introduction

It is our growing understanding that planetary waves, gravity waves and tides dominate the structure and dynamics of the mesosphere and lower thermosphere (MLT) region. Long-term observations are therefore important for quantifying seasonal variability of this region as a function of latitude, and for investigating the primary causes of the variability. Satellite measurements provide excellent geographic coverage usually over a several year period, but, due to orbital constraints, the measurements are naturally limited to sampling at certain local times (e.g., Clancy and Rusch, 1989; Shepherd et al., 1998). On the other hand, rocket-borne sampling of the MLT region can be made from any latitude (providing there is a suitable launch facility available), but the data are of very limited duration. In contrast, ground-based observations offer an economical and very important method for routine remote sensing studies of the upper atmosphere. Although these measurements are subject to changes in the viewing conditions (due to adverse weather), long-term observations from a well chosen mountain site provide an excellent opportunity for seasonal studies of the MLT region.

As early as the International Geophysical Year (IGY) ground-based investigations have been carried out to study the seasonal variability in the mesospheric nightglow emissions. Initial investigations revealed strong latitudinal and seasonal variations in the mesospheric OI (557.7 nm), Na (589.3 nm), and the near infrared OH Meinel nightglow emission intensities which originate from well defined layers in the upper mesosphere (e.g.,

* Corresponding author. Tel.: +1 435 797 3919; fax: +1 435 713 2992.
E-mail addresses: mtaylor@cc.usu.edu (M.J. Taylor), ataori@aries.wernet.in (A.K. Taori).
[1] Present address: Aryabhatta Research Institute of Observational Sciences, Nainital, India.

0273-1177/$30
doi:10.1016/j.asr.2005.05.111

Roach and Smith, 1967; Wiens and Weill, 1973; Fukuyama, 1977). Longer-term observations have also revealed semi-annual, annual and quasi-biennial oscillations in these data sets, the characteristics of which alter significantly with latitude. Furthermore, modeling and observational studies of the seasonal variability of the OH Meinel band emission intensity have shown that at low- and mid-latitudes vertical diffusion (due primarily to small-scale gravity wave breaking) can be large, leading to a semi-annual-type oscillation while, at higher latitudes much stronger vertical advection leads to an annual-type oscillation (e.g., Le Texier et al., 1987). Variations of the vertical diffusion and residual circulation in the MLT region, both induced by gravity wave breaking, are also likely causes of mesospheric OI (557.7 nm) seasonal variations at mid-high latitudes (e.g., Garcia and Solomon, 1985; Liu and Roble, 2004).

In addition to measuring the mesospheric emission intensities it is also possible to use optical techniques to determine the temperature of the mesosphere at the height of the emission layers. Long-term investigations of mesospheric temperature using a variety of optical instrumentation ranging from simple photometry to interferometry and nowadays CCD imaging and resonant lidar sounding techniques continue to be conducted (e.g., Niciejewski and Killeen, 1995; She et al., 2000; States and Gardner, 2000; Bittner et al., 2000; Espy and Stegman, 2002). The majority of these measurements have been made from mid- and high latitude sites and have revealed a strong annual-oscillation in middle atmosphere temperatures with some evidence for an additional, but small, semi-annual component at mid-latitudes. In contrast, long-term, ground-based measurements of mesospheric temperature at low- and equatorial latitudes are exceedingly few (e.g., Takahashi et al., 1995; Friedman, 2003) and the seasonal structure and variability of the MLT region has yet to be fully quantified.

This paper utilizes ground-based observations of the nightglow emissions from the US Air Force AEOS high altitude facility located at the summit of Haleakala Crater, Maui, Hawaii (20.8°N, 156.2°W, 2970 m), which affords excellent seeing conditions throughout the year. The present work focuses on long-term observations of the mesospheric OH M (6,2) and O_2 (0,1) atmospheric band temperature and their variability over a 25-month (encompassing 2002–2003). The measurements were made using the CEDAR Mesospheric Temperature Mapper (MTM) and show a clear semi-annual-oscillation in the nocturnal temperatures in both data sets.

2. Instrumentation and observations

The Mesospheric Temperature Mapper (MTM) was developed at Utah State University (USU) in 1997 with support from the National Science Foundation (NSF) Coupling, Energetics and Dynamics of Atmospheric Regions (CEDAR) program. The MTM is a high performance, solid state imaging system capable of determining variations in the intensity and rotational temperatures of two upper mesospheric near infrared nightglow emissions: the OH M (6,2) band (peak altitude ~87 km), and the O_2 (0,1) atmospheric band emission (peak altitude ~94 km), both of which exhibit well defined half-widths of ~8–10 km (e.g., Donahue et al., 1973; Baker and Stair, 1988). The MTM utilizes a large format 1024×1024 pixel CCD array coupled to a 90° circular field of view telecentric lens system. The detector is cooled to −50 °C using a two-stage Peltier system assisted by a closed cycle liquid refrigeration unit providing very low noise operational characteristics (dark current ~0.1 e^-/pixel/s). Sequential observations are made using narrow band ($\Delta\lambda \sim 1.2$ nm) interferences filters centered at 840 and 846.5 nm for the OH M (6,2) band and 866 and 868 nm for the O_2 (0,1) atmospheric band measurements followed by a background sky measurement at 857 nm. Each filter is exposed for 60 s duration resulting in a cadence of ~5.5 min. To optimize the temperature determinations the CCD data are binned 8×8 on the chip to form a 128×128 super-pixel image with a resultant zenithal foot print of $\sim 0.9 \times 0.9$ km per super-pixel. Rotational temperatures are then computed separately using the ratio method as described eloquently by Meriwether (1984). The precision of the emission intensity measurements is better than 0.5% (for an individual image) and the derived rotational temperatures are better than 1–2 K (in 3 min) or 0.5 K in 1 h (Pendleton et al., 2000). Recent comparisons of the MTM temperature data with coincident Na lidar and satellite borne temperature measurements indicates that the MTM results are accurate to about ±5 K for both the OH and the O_2 data when referenced to their nominal emission altitudes of 87 and 94 km, respectively (e.g., Pendleton et al., 2000; von Savigny et al., 2004; Zhao et al., 2005). Of key importance to this investigation is the inherent linearity and stability of the MTM which provides an additional capability for high-precision seasonal investigations of mesospheric temperature variability (Taylor et al., 2001).

Since November 2001 the MTM has operated near-continuously at Maui, HI as part of the Maui-MALT program which is a jointly sponsored initiative between the US Air Force Office of Scientific Research (AFOSR) and the National Science Foundation (NSF). Autonomous observations are made on a routine basis centered on the new moon period (for ~22 nights per month) in coordination with a suite of optical and radar measurements to investigate the dynamics of the mesosphere and lower thermosphere (MLT) region at low-latitudes over the central Pacific Ocean. Recent related results describing coordinated measurements using the MTM with a co-located meteor radar and an Na wind temperature

lidar system are given in Taori et al. (2005) and Zhao et al. (2005).

3. Results

To date over 467 nights of quality data have been collected from Hawaii by the MTM over a 25 month period from October 2001 to January 2004. Further measurements are continuing at Maui but the data have yet to be incorporated into this analysis. Fig. 1 plots the nightly mean OH and O_2 temperatures for all 467 nights when good data were collected for durations of more than 4 h. A 4 h cut off was chosen to help minimize the contributions of tides to the mean night-time temperature determinations (and are discussed herein), as employed by previous observers (e.g., Takahashi et al., 1995; She and Lowe, 1998). The data are plotted in UT day number and start late in October 2001 (UT day 295). To aid the comparison, both plots use the same scales. A characteristic of the MTM data is that the nocturnal variability in both emissions is dominated invariably by tidal effects that produce temperature changes of typically 5–20 K during the course of any given night (Pendleton et al., 2000; Taori et al., 2005). In both plots the "error bars" show the standard deviation in the mean of the nightly temperature distribution for each emission, which, due to the high precision in the individual measurements, is due mainly to geophysical variability. This is illustrated in Fig. 2 which shows the raw (5.5-min sample interval) OH and O_2 temperatures derived from intensity data recorded on July 5, 2003 (UT day 186). On this night both temperature plots

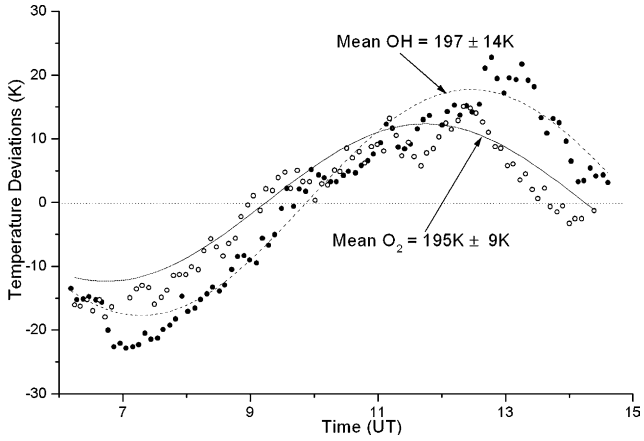

Fig. 2. Example showing typical temperature variability in the OH and O_2 data as observed on July 5, 2003 (UT day 186). The nocturnal variability is driven mainly by long-period tidal forcing with superposed smaller-scale gravity waves.

show a clear signature of a long-period oscillation (possibly due to the semi-diurnal tide), with amplitudes of ~10 K (O_2) and 15 K (OH). This is indicated by the simple least-squares fit curve to each data set using a fixed 12 h periodicity. Superimposed on the long-period variation are several smaller amplitude perturbations due primarily to shorter period gravity waves. The mean nocturnal temperatures for the OH and O_2 data were 197 ± 14 and 195 ± 9 K, where the uncertainties are clearly driven by the tide-like perturbation.

Returning to Fig. 1, it is evident that the data set is well populated with only short data gaps (of a few days duration) occurring every full moon period. However, during the April–May 2002 period (day numbers ~460–520) the MTM measurements were compromised

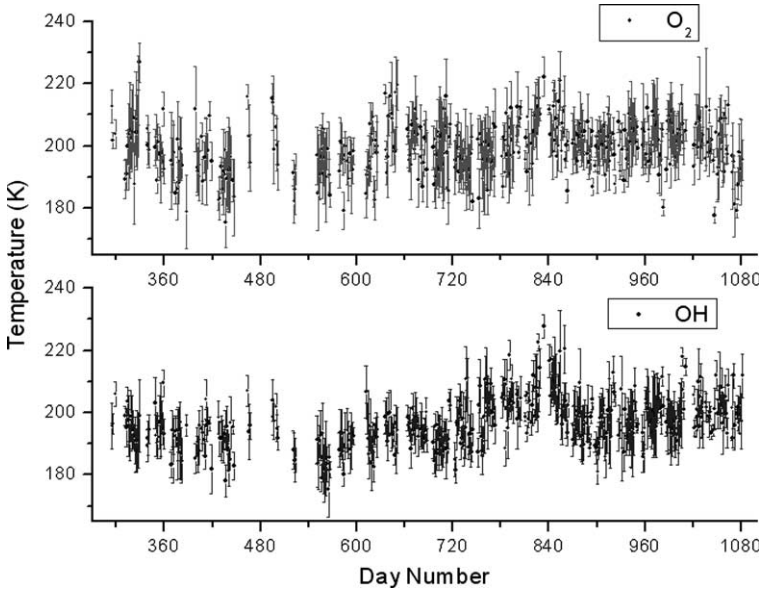

Fig. 1. Ensemble of 467 nightly mean measurements of mesospheric OH and O_2 temperatures as recorded from Maui (20.8°N) during the period October 2001–January 2004. The individual "error bars" represent the standard deviations for each data night.

by an intermittent camera cooling problem. Nevertheless, the data show that during this ~2-yr period, the O_2 temperatures ranged from typically 185 to 215 K (mean 199.6 K) while the OH temperatures exhibited a slightly broader range (~175–220 K), but a similar mean value of 196.9 K . Evident in both data sets is a long-period oscillation in temperature which exhibits a distinct peak around day 840 and a second peak of smaller amplitude (around day 660), suggestive of a seasonal oscillation of periodicity ~0.5 yr. Unfortunately, the limited data recorded during the spring 2002 restricts the detection of an additional (expected) peak around day 480, yet the few available measurements during this period do suggest such a feature in both the OH and O_2 data sets.

To help quantify this apparent seasonal variability in mesospheric temperatures, Fig. 3 re-plots the data for Fig. 2 folded into a 1-yr interval. In this format some nights contain more than one data point while other nights help fill in the April–May 2002 data gap. The form of the long-period oscillation is now immediately evident exhibiting a marked double humped structure with distinct peaks around the spring (UT day 95) and fall (UT day 275) period implying a semi-annual-type oscillation. A simple least squares sinusoidal fit to the O_2 data indicates a near symmetrical perturbation of amplitude 5.7 ± 0.4 K and a periodicity 182 ± 7 days. This is shown by the superimposed solid curve in the upper plot. A least-squares analysis of the OH data (lower plot) indicates very similar mean amplitude of 5.8 ± 0.6 K and an almost identical wave periodicity (181 ± 6 days) to that determined independently from the O_2 data. However, the OH oscillation is not as symmetrical and the data exhibit significantly larger perturbation amplitude in the spring (~10 K) than during the fall period (~3 K).

To investigate this oscillation further, Fig. 4 presents a composite (1-yr folded) plot the OH M (6, 2) and O_2 (0, 1) atmospheric band intensities derived from the MTM image data for the same period. A strong seasonal variation is again evident in both data sets with a conspicuous peak in the spring and a smaller amplitude peak in the fall period in clear synchronization with the temperature data of Fig. 3. Least-squares estimates of the perturbation amplitudes (not shown) indicate ~8–9% for both the OH and O_2 data sets. However, in this case the O_2 intensity data exhibit a larger amplitude perturbation during the spring-time as compared with the OH data. Together these two data sets provide new evidence for the presence of a coherent mesospheric oscillation of period ~180 days and significant amplitude in both the OH and O_2 emission intensity and temperature data sets during this ~2-yr period.

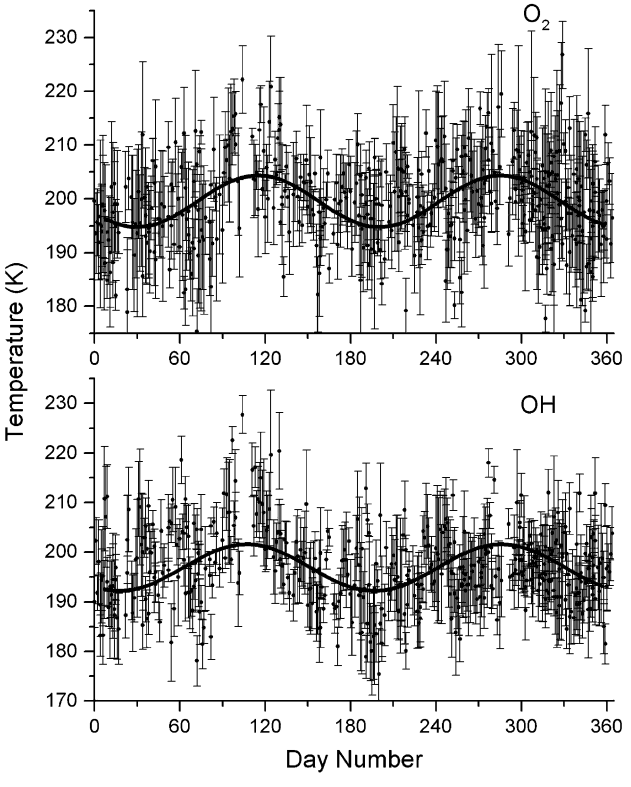

Fig. 3. Composite plot showing the data of Fig. 1 folded into a 1-yr period. Both OH and O_2 data sets show a well-defined semi-annual oscillation (indicated by the fitted curves) with maxima during the spring and fall periods. Note the spring peak has a larger amplitude than the fall peak.

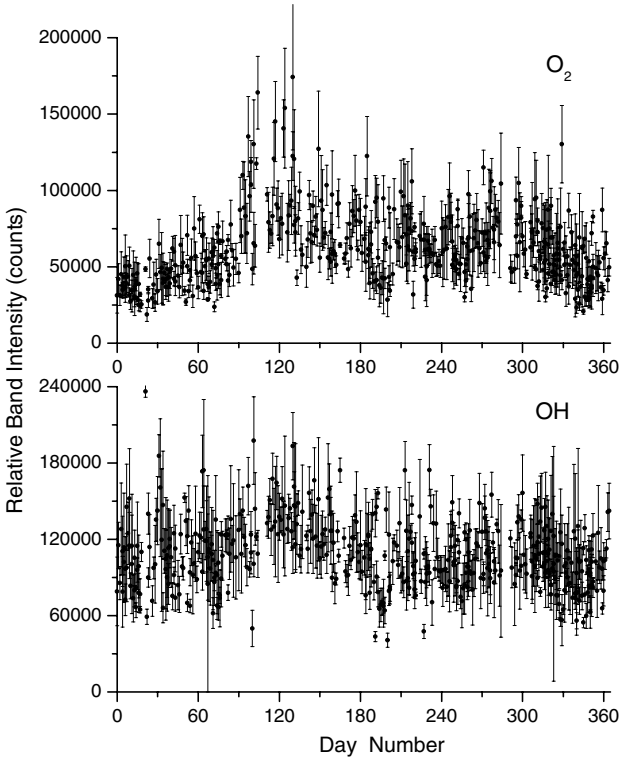

Fig. 4. Corresponding plot to Fig. 3 showing the 1-yr folded relative band intensity data for the OH and O_2 emissions. A similar periodicity semi-annual-oscillation is again evident in both data sets, with a larger peak occurring during the spring time.

4. Discussion

The long-period perturbation reported herein is highly suggestive of a semi-annual-oscillation (SAO) in temperature. To date, there have been exceedingly few measurements of the SAO signature in mesospheric temperature. Our observations help characterize the form of this oscillation as detected at low-latitudes (~21°) in the northern hemisphere. In particular, independent OH and O_2 temperature estimates at two different mean altitudes (~87 and 94 km) in the upper mesosphere both indicate a semi-annual-oscillation in temperature of amplitude ~5–6 K. This is equivalent to a percentage oscillation of ~7–8% for a mean annual temperature around 200 K. However, our data also suggest that the spring-time perturbation is significantly larger than that observed during the fall period as evident in both the temperature and intensity data sets.

As far as we are aware the only previous ground-based measurements of the SAO were reported by Takahashi et al. (1995). They presented results of a 5-yr series of Southern Hemisphere measurements from two sites in Brazil; one located near the equator at Fortaleza (3.9°S) and the other at Cachoeira Paulista (22.7°S), at a similar latitude to our measurements in Hawaii. At both sites they used a tilting-filter photometer to sequentially measure three nightglow emissions, the NIR OH (9,4) Meinel band, the Na (589.3 nm) line emission (peak height ~90 km) and the OI (557.7 nm) green line emission (peak height ~96 km). Fig. 5 summarizes the results of their OH rotational temperature measurements from these two sites. The top panel plots the temperature data from Fortaleza which exhibits a marked semi-annual-oscillation of fitted periodicity 182.5 days and amplitude ~8.5 K. This is illustrated by the solid curve which connects monthly mean temperatures derived from the 5-yr folded data set. The lower panel shows the corresponding data for Cachoeira–Paulista which indicates a similar periodicity oscillation but of significantly lower amplitude (3.5 K). Their OH intensity data (not shown here) also exhibited a similar characteristic behavior with the largest amplitude for the semi-annual oscillation occurring closer to the equator. As similar periodicity oscillations were also evident in their Na and OI airglow emission data (which originate at higher altitudes within the MLT region) Takahashi et al. (1995) concluded that their data were the signature of a predominant semi-annual-oscillation evident in the upper mesospheric emissions and temperatures in the equatorial region. Our measurements are in close agreement with their results but our observed temperature perturbation amplitude (~5–6 K) falls in between their two reported values.

Previous measurements of the SAO in mesospheric temperature were reported by Clancy and Rusch (1989) using the Solar Mesospheric Explorer (SME) satellite data. The SME satellite observed scattering of ultraviolet light in the earth's limb to derive temperatures over the height range 58–90 km with a resolution of ~3 km. Tables of results are available for comparison with our ground-based airglow measurements. Fig. 6 shows the SAO signature determined by SME for three consecutive sample heights in the upper mesosphere, 83, 86.5, and 90 km (maximum available height), for 20°N latitude. The SAO signature is shown to be largest at 90 km; exhibiting an amplitude of ~15 K that reduces down to ~5 K at the 83 km level. At the approximate peak of the OH emission (86.5 km) the SME data indicate an amplitude of ~10 K which is somewhat larger that our observed value of ~6 K (for both OH and O_2 data sets). However, as our intensity data (and hence the temperature determinations) are height weighted over the nominal ~8–10 km OH and O_2 layer thickness the agreement is very promising. This said, the SME data do not indicate any significant asymmetry between the spring and fall maxima as we have reported herein. In contrast, close inspection of the ground-based temperature data from Fortaleza (3.9°S) reported by Takahashi et al., 1995 (see Fig. 5) shows some evidence

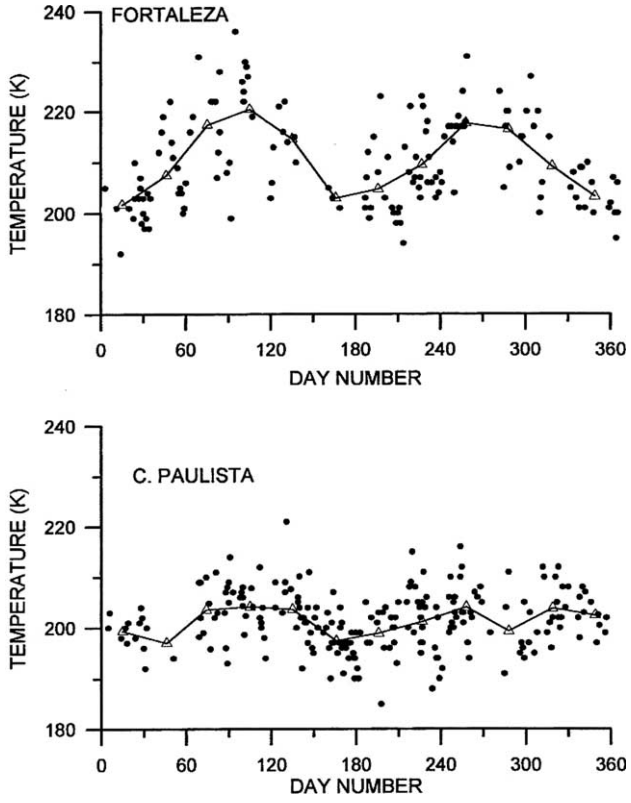

Fig. 5. The seasonal variations in OH rotational temperature reported by Takahashi et al., 1995, (This figure is reproduced with kind permission of the author). The top panel shows the temperature data for Fortaleza (3.9°S) while the bottom panel presents the data for Cachoeira–Paulista (22.7°S). In each case the solid curve plots the monthly averaged data.

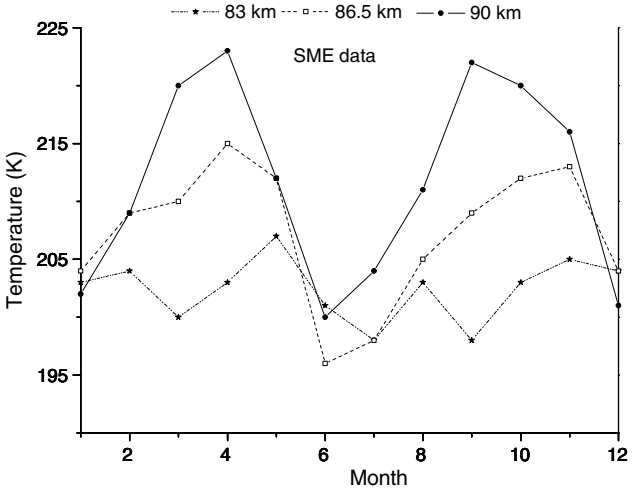

Fig. 6. Solar Mesosphere Explorer (SME) data for 20°N latitude for three mean altitudes in the upper mesosphere (derived from tabulations by Clancy and Rusch (1989)). Note the symmetry of the data and the apparent growth in amplitude with altitude.

for a larger amplitude peak in the spring in support of our measurements. Furthermore, asymmetry in seasonal mesospheric temperatures has also been observed in an ensemble of rocket soundings obtained from a number of sites at low- and equatorial latitudes as reported by Cole and Cantor (1978). However, the Cachoeira–Paulista data (23°S), which are closer to our latitude of observations, are less well defined and do not show any significant asymmetry.

Clancy and Rusch (1989) concluded that the temperature oscillations detected by the SME were presumably related to the well-established semi-annual-oscillation in the equatorial mesospheric mean wind field. Previous measurements of the SAO signature in mesospheric winds also indicate a strong asymmetry with the first peak (spring) significantly larger than the second (fall) peak (e.g., Hirota, 1978; Hamilton, 1982; Delisi and Duknerton, 1988). Thus, it is not surprising to see a similar feature in the mesospheric temperature data. In summary, the high quality of our large ground-based data set (obtained over a >2-yr period) strongly supports the existence of an asymmetry in the SAO as evident in both intensity and temperature data from two height-separated airglow emissions.

Although not discussed by Clancy and Rusch (1989), the possibility of tidal aliasing affecting the SAO structure as determined using the SME data has been raised by Garcia et al. (1997). As the SME data are sampled around local noon there is the possibility that the diurnal tidal perturbation (which dominates the MLT region at low-latitudes) could significantly affect the observed amplitude and phase of the SAO signature. As our temperature measurements at Maui, HI were also made over a limited nocturnal period (typically 4–9 h centered on local midnight), there is a possibility that tidal aliasing will also contribute to the measured SAO signature reported here. However, the local time of the SME sampling (~3 pm) and our MTM measurement (mean ~10 pm to 2 am) is about 9 h apart. Hence, the SAO signals from these two measurements would be expected to be out of phase if diurnal tidal aliasing were the main contributor to the measured SAO signal. The MTM and SME temperature data of Figs. 3 and 6, respectively, both show positive (i.e., in phase) peaks in April and October at 20°N around 87 km altitude. This therefore suggests that the major cause of the observed SAO signal is not tidal aliasing. We are further investigating the effects of the diurnal tide on our seasonal nocturnal temperature data set using the National Center for Atmospheric Research (NCAR) thermosphere–ionosphere–mesosphere–electrodynamics general circulation model (TIME-GCM) estimates of the tidal amplitudes and phases. The results of this work will be reported at a later date.

Finally, an important new data set on low-latitude mesospheric temperatures has recently been reported by Friedman (2003). Potassium resonance lidar observations were made over an ~22 month period (April 2001–February, 2003) from Arecibo Observatory, Puerto Rico (18.35°N) at a very similar latitude to our Hawaiian measurements and also overlapping well in time with our MTM data. An ensemble of 74 nights of lidar measurements showing height-resolved temperatures over the altitude range ~80–105 km was used to investigate the seasonal variability of the temperature and altitude of the mesopause. Although Friedman does not discuss the nature of the seasonal variability, examination of the lidar data (his Fig. 2) does show evidence of a semi-annual variability in temperature at altitudes below ~95 km that evolves more into an annual-type oscillation at higher altitudes. Our OH temperature data (mean height ~87 km) are in good qualitative agreement with the lidar measurements but a comparison with the O_2 data (mean height ~94 km) was much poorer. However, there are still conspicuous gaps in the lidar data ensemble around the spring (mid-March through mid-April) and fall (mid-September through mid-October) periods, which currently limit a more quantitative study of the SAO spring and fall amplitudes. A detailed comparison between the lidar and MTM data is planned when there are additional lidar data available around the equinox periods.

5. Conclusion

This paper presents new measurements of mesospheric temperature at low-latitudes recorded over a 25 month interval encompassing 2002–2003. Data from two airglow emissions independently show a clear oscil-

lation in mesospheric temperature and OH and O_2 emission intensity with a characteristic period of ~180 days. The first peak occurs around UT day 95 while the second peak occurs about UT day 280, consistent with a semi-annual-type oscillation. Measurements of the mean amplitude of the temperature perturbation yield ~5–6 K for both emission layers and ~8–9% for their fractional intensity variations. A significant asymmetry was also found with larger amplitudes for the temperature and intensity perturbations occurring during the spring. Measurements of this type of oscillation in mesospheric temperature are rare and the characteristics of seasonal variation compare well with those previously reported in the mesospheric wind field.

Acknowledgements

We are most grateful Dr. P. Kervin, Director of the Maui AEOS Facility, for supporting the Maui-MALT measurements program. We kindly acknowledge the Boeing support staff and, in particular, wish to thank R. Taft and S. AhYou for their unstinting help with the remote operation of our MTM imager. This research was conducted as part of a joint program between the Air Force Office of Scientific Research (AFOSR) and the National Science Foundation (NSF). Financial support for the measurements and data analyses was provided by NSF Grant ATM 0003218. As part of this research, A. Taori was supported as a CEDAR Post Doctoral Fellow under NSF Grant ATM 0134150.

References

Baker, D.J., Stair Jr., A.T. Rocket measurements of the altitude distributions of the hydroxyl airglow. Phys. Script. 37, 611–622, 1988.

Bittner, M., Offermann, D., Graef, H.H. Mesopause temperature variability above a midlatitude station in Europe. J. Geophys. Res. 105, 2045–2058, 2000.

Clancy, R.T., Rusch, D.W. Climatology and trends of mesospheric (55–90 km) temperatures based upon 1982–1986 SME limb scattering profiles. J. Geophys. Res. 94, 3377–3393, 1989.

Cole, A.E., Cantor, A.J., Air force reference atmospheres, project 6670. Tech. Rep. AFGL-TR-78-0051, Meteorol. Div., Air Force Geophys. Lab. Hanscom, Mass, 1978.

Delisi, D.P., Duknerton, T.J. Seasonal variation of the semiannual oscillation. J. Atmos. Sci. 45 (19), 2772–2787, 1988.

Donahue, T.M., Guenther, B., Thomas, R.J. Distribution of atomic oxygen in the upper atmosphere deduced from OGO 6 airglow observations. J. Geophys. Res. 78, 6662–6669, 1973.

Espy, P.J., Stegman, J. Trends and variability of mesospheric temperature at high latitudes. Phys. Chem. Earth 27, 543–553, 2002.

Friedman, J.S. Tropical mesopause climatology over the Arecibo observatory. Geophys. Res. Lett. 30 (12), 1642, doi:10.1029/2003GL016966, 2003.

Fukuyama, K. Airglow variations and dynamics in the lower thermosphere and upper mesosphere-II. Seasonal and long term variations. J. Atmos. Terr. Phys. 39, 1–14, 1977.

Garcia, R.R., Dunkerton, T.J., Lieberman, R.S., Vincent, R.A. Climatology of the semiannual oscillation of the tropical middle atmosphere. J. Geophys. Res. 102, 26019–26032, 1997.

Garcia, R.R., Solomon, S. The effect of breaking gravity waves on the dynamics and chemical composition of the mesosphere and lower thermosphere. J. Geophys. Res. 90, 850–3868, 1985.

Hamilton, K. Rocketsonde observations of the mesospheric semiannual oscillation at Kwajalein. Atmos. Ocean 20, 281–286, 1982.

Hirota, I. Equatorial waves in the upper stratosphere and mesosphere in relation to the semi-annual oscillation of the zonal wind. J. Atmos. Sci. 95, 714–722, 1978.

Le Texier, H., Solomon, S., Garcia, R.R. Seasonal variability of the OH Meinel bands. Planet. Space Sci. 35 (8), 977–989, 1987.

Liu, H.-L., Roble, R.G. Dynamical processes related to the atomic oxygen equinox transition. J. Atmos. Solar Terr. Phys 66, 769–779, 2004.

Meriwether, J.W. Ground based measurements of mesospheric temperatures by optical means. MAP Handbook 13, 1–18, 1984.

Niciejewski, R.J., Killeen, T.L. Annual and semi-annual temperature oscillations in the upper mesosphere. Geophys. Res. Lett. 22, 3243–3246, 1995.

Pendleton Jr., W.R., Taylor, M.J., Gardner, L.C. Terdiurnal oscillations in OH Meinel rotational temperatures for fall conditions at northern mid-latitude sites. Geophys. Res. Lett. 27, 1799–1802, 2000.

Roach, F.E., Smith, L.L. The worldwide morphology of the atomic oxygen nightglows. in: McCormac, B.M. (Ed.), Aurora and Airglow. Reinhold, New York, pp. 29–39, 1967.

She, C.Y., Lowe, R.P. Seasonal temperature variations in the mesopause region at mid latitude: comparison of lidar and hydroxyl rotational temperatures using WINDII/UARS OH profiles. J. Atmos. Sol. Terr. Phys. 60, 1573–1583, 1998.

She, C.Y. et al. Eight year climatology of nocturnal temperature and sodium density in the mesopause region (80 to 105 km) over Fort Collins (41°N, 105°W). Geophys. Res. Lett. 27, 3289–3292, 2000.

Shepherd, G.G., Roble, R.G., Zhang, S.P., McLandress, C., Wines, R.H. Tidal influence on mid latitude airglow: comparison of satellite and ground based observations with TIME-GCM predictions. J. Geophys. Res. 103, 14741–14751, 1998.

States, R.J., Gardner, C.S. Thermal structure of the mesopause region (80 – 1–5 km) at 40°N latitude. Part I: seasonal variations. J. Atmos. Sci. 57, 66–77, 2000.

Takahashi, H., Clemesha, B.R., Batista, P.P. Predominent semi-annual oscillation of the upper mesospheric airglow intensities and temperatures in the equatorial region. J. Atmos. Terr. Phys. 57 (4), 407–414, 1995.

Taori, A., Taylor, M.J., Franke, S. Terdiurnal wave signatures in the upper mesospheric temperature and their association with the wind fields at low-latitudes (20°N). J. Geophys. Res. 110, D09S06, doi:10.1029/2004JD004564, 2005.

Taylor, M.J., Pendleton Jr., W.R., Liu, H.L., She, C.Y., Gardner, L.C., Roble, R.G., Vasoli, V. Large amplitude perturbations in mesospheric OH Meinel and 87-km Na lidar temperatures around the autumnal equinox. Geophys. Res. Lett. 28 (9), 1899–1902, 2001.

von Savigny, C., Eichmann, K.-U., Llewellyn, E.J., Bovensmann, H., Burrows, J.P., Bittner, M., Höppner, K., Offermann, D., Taylor, M.J., Zhao, Y., Steinbrecht, W., Winkler, P. First near-global retrievals of OH rotational temperatures from satellite-based Meinel band emission measurements. Geophys. Res. Lett. 31 (15), doi:10.1029/2004GL020410, 2004.

Wiens, R.H., Weill, G. Diurnal, annual and solar cycle variations of hydroxyl and sodium nightglow intensities in the Europe–Africa sector. Planet Space Sci. 21, 1011–1027, 1973.

Zhao, Y., Taylor, M.J., Chu, X. Comparison of Na lidar and mesospheric nightglow temperature measurements and the effects of tides on the emission layer heights. J. Geophys. Res. 110, D09S07, doi:10.1029/2004JD005115, 2005.